Prepared for submission to JHEP

Machine Learning for Survival Analysis: A New Approach

D. Dooling P. Green A. Kim D. Scroggin L. Stevens J. Webster

Innovative Oncology Business Solutions,
4901 Lang Ave NE,
Albuquerque, NM 87109, USA

E-mail: ddooling@innovativeobs.com, pgreen@innovativeobs.com, akim@innovativeobs.com, dscroggin@innovativeobs.com, lstevens@innovativeobs.com, jwebster@innovativeobs.com

Abstract: We have applied a little-known data transformation to subsets of the Surveillance, Epidemiology, and End Results (SEER) publically available data of the National Cancer Institute (NCI) to make it suitable input to standard machine learning classifiers. This transformation properly treats the right-censored data in the SEER data and the resulting Random Forest and Multi-Layer Perceptron models predict full survival curves. Treating the 6, 12, and 60 months points of the resulting survival curves as 3 binary classifiers, the 18 resulting classifiers have AUC values ranging from .765 to .885. Further evidence that the models have generalized well from the training data is provided by the extremely high levels of agreement between the random forest and neural network models predictions on the 6, 12, and 60 month binary classifiers.

Contents

1 Introduction and Background

Opportunities are emerging in many indutries today to develop and deploy services that cater to individual needs and preferences. Music afficianados can create their own radio stations tailored to their individual tastes from Pandora[1], bibliophiles can receive highly trustworthy book recommendations from goodreads.com[2], and Google will provide directions between any two points, giving options such as mode of transportation and as well as warnings of delays in realtime.[3] These individualized services share many common features. In particular, they leverage large databases of aggregated information to learn and extract information relevant to individuals. Extracting actionable information from data is changing the fabric of modern business. A class of techniques that transforms data into actionable information goes by the name of Machine Learning [1]. Machine Learning has recently become a popular method to answer questions and solve problems that are too complex to solve via traditional methods.

The primary objective of this study is to show how machine learning methods can be trained with data in cancer registries to produce personalized survival prognosis curves, but the methods presented below can be applied to any type of survival data. Traditionally, cancer survival curves have been estimated using Kaplan-Meier methods [2]. Kaplan-Meier methodology also uses large datasets to make predictions, but the resulting information is not personal; the resulting curves are summaries for a population and not necessarily relevant or particularly accurate for any given individual. This propery of Kaplan-Meier methods is exacerbated when dealing with heterogeneous populations. The methods described below also take full advantage of all relevant aggregate information, but are able to provide personalized survival curves relevant to individual subjects. This objective is in keeping with the recent movement in medicine known as Predictive, Preventive and Personalized Medicine (PPPM), which aims to leverage increasing amounts of health related data to maximize quality of care and to intelligenctly eliminate inefficient and unecessary use of resources [3]. This capability of providing individualized survival curve prognosis is a direct result of the recent advances in computing power and machine learning algorithms, and similar methodology is becoming commonplace in many industries. These techniques are now infiltrating the healthcare industry, in spite of some of the data aggregation challenges posed by the Health Insurance Portability and Accountability Act (HIPPA) of 1996. This study makes use of a freely available data source that circumvents the restrictions imposed by HIPPA.

The Surveillance, Epidemiolgy, and End Results (SEER) Program of the National Cancer Institute (NCI) has been collecting data because intuitively researchers feel confident that this data will eventually allow researches to detect information crucial to patients and providers including the relationships between the types of data collected (demographic as

[1] Pandora Internet Radio - Listen to Free Music You'll Love, http://www.pandora.com/ (accessed 27 Jan 2016)

[2] Share Book Recommendations With Your Friends, Join Book Clubs, Answer Trivia, https://www.goodreads.com/ (accessed 27 Jan 2016)

[3] Google Maps, https://goo.gl/lD7Jwf (accessed 27 Jan 2016)

well as staging information, treatment and disease characteristics) and the survival outcomes. Though these relationships evade capture by traditional methods, it is possible to surface them with two machine learning techniques known as *Random Forests* and *Neural Networks*. As will be demonstrated in section (6.2), these two methods produce very similar results when applied to the SEER dataset, and are based on almost diametrically opposed learning philosophies, which lends confidence in the validity of the results.

The Surveillance, Epidemiolgy, and End Results (SEER) Program of the National Cancer Institute (NCI) is the most recognized authoritative source of information on cancer incidence and survival in the United States. SEER currently collects and publishes cancer incidence and survival data from population-based cancer registries covering approximately 28 percent of the US population.

Quoting directly from the SEER website [4]:

> The SEER program registries routinely collect data on patient demographics, primary tumor site, tumor morphology and stage at diagnosis, first course of treatment, and follow-up for vital status. This program is the only comprehensive source of population-based information in the United States that includes stage of cancer at the time of diagnosis and patient survival data. The mortality data reported by SEER are provided by the National Center for Health Statistics. The population data used in calculating cancer rates is obtained periodically from the Census Bureau. Updated annually and provided as a public service in print and electronic formats, SEER data are used by thousands of researchers, clinicians, public health officials, legislators, policymakers, community groups, and the public.

One characterstic of the SEER data that is shared by many datasets in the medical field goes by the name of "censored data." Observations are labeled censored when the survival time information is incomplete. The SEER data contains the number of months each patient survived, as well as an indicator variable showing whether or not the patient is still alive at the end of the data collection period. Methods to deal effectively with this kind of "right-censored data" include Kaplan-Meier curves and Cox Proportional Hazard models [2]. The Kaplan-Meier techniques only give estimates for cohorts of patients and are not applicable for predicting the surival curve for a single patient, and the Cox Proportional Hazard models require a fairly restrictive set ot assumptions to be satisifed in order to yield reliable results.

Previous work applying machine learning methods to subsets of the SEER data include creative attempts to deal with the problems presented by "right-censored data." Shin et al. [5] use semi-supervised learning techniques to predict 5 year survival, essentially imputing values for SEER records where the survival months infomation is censored at a value less than 5 years. Zolbanin et al. [6] investigate the effects of comordbidities; i.e., patients with two different cancer diagnosises, but their treatment of the censored data underestimates the survival probabilities. All records representing patients who survived at least 60 months as well as all those who died earlier than 60 months were considered, but patients alive

prior to 60 months but censored out of the study before 60 months were not included. This treatment biases the data and the predictions, leading to overly pessimistic survival probablilites predicted by the models.

Previous work applying machine learning methods based on decision trees to survival data in general have a long history, starting with Gordon et al. [7]. A summary of more recent developments concerning *survival trees* is provided by Bou-Hamad et al. [8]. These methods focus on altering the splitting critieria used in decision tree growth to account for the censoring, and use 1958 Kaplan-Meier methods at the resulting nodes for prediction purposes. These methods do not generalize to non-tree-based machine learning algorithms, though Ishwaran et al. have extended the methodology to *random survival forests*, ensembles of *survival trees* [9].

IOBS has applied a little-known technique to transform the SEER data to make it amenable to more powerful machine learning methods. Instead of modifying existing learning algorithms in drastic ways, we focus attention on the input data. This approach allows for different machine learning algorithms to use the same data with no modification. The essential idea is to recast the problem to an appropriate discrete classification problem instead of a regression problem (predicting survival months). Treating months after diagnosis as just another discrete feature, the SEER data (or any other right-censored data) can be transformed to make predictions for the hazard function (probability of dying in the next month, given that the patient has not yet died). The full survival function can then be derived from the hazard function.

This paper is organized as follows. In section (2) we introduce the subsets of the SEER data used for this study, and present survival curves computed from traditional methods based on this data for the three cancer types *lung*, *breast*, and *colon*. In section (3) we present the essential methodology of this work, the data trasnformation that allows censored survival data to be used as input to exisiting machine learning classifiers. Section (5) presents the details of the trained models, including some some subtleties arising from the data transformation pertaining to the partition into training and test datasets. The method of deriving binary classifiers from the models' predictions for the survival curves is presented. In this paper, we have constructed binary classifiers corresponding to 6, 12, and 60 months, as these are standard metrics in cancer survival prognosis. In section (6) we present the evaluations of the trained models. The performance metrics are the 18 AUC curves associated with the 6, 12, and 60 month survival binary classifiers for the two models associated with each cancer type. We also present additional evidence supporting validity of the predictions by computing the levels of agreement between the random forest and neural network models for each of the 18 binary classifiers and find striking agreement. In section (7) we provide urls for 6 web applications that use the trained models to predict individual cancer survival prognosis curves. These apps are hosted on the popular Heroku website, and allow for exploration of the nonlinear relationships between the input features and resulting survival prognosis. It is exactly these kinds of tools that are the goal of Predictive, Preventitive and Personalized Medicine. Finally, we present avenues for future research in section (8).

2 Data acquisition

We use the publically available 1973-2012 SEER incidence data files corresponding to colon, breast and lung cancer contained in the list below. SEER requires that researchers submit a request for the data, which includes an agreement form. Detailed documentation explaining the contents of both the incidence data files used in this study as well as a data dictionary for the 1973-2012 SEER incidence data files are available without the need to register or submit a data request [10].

- incidence\yr1973_2012.seer9\COLRECT.txt
- incidence\yr1973_2012.seer9\BREAST.txt
- incidence\yr1973_2012.seer9\RESPIR.txt
- incidence\yr1992_2012.sj_la_rg_ak\COLRECT.txt
- incidence\yr1992_2012.sj_la_rg_ak\BREAST.txt
- incidence\yr1992_2012.sj_la_rg_ak\RESPIR.txt
- incidence\yr2000_2012.ca_ky_lo_nj_ga\COLRECT.txt
- incidence\yr2000_2012.ca_ky_lo_nj_ga\BREAST.txt
- incidence\yr2000_2012.ca_ky_lo_nj_ga\RESPIR.txt
- incidence\yr2005.lo_2nd_half\COLRECT.txt
- incidence\yr2005.lo_2nd_half\BREAST.txt
- incidence\yr2005.lo_2nd_half\RESPIR.txt

2.1 Data preparation and preprocessing

A great deal of data munging is necessary before using these SEER incidence files as input into machine learning algorithms. A preprocessing step common to each of the three cancer types studied involves the `STATE-COUNTY RECODE` variable. The `STATE-COUNTY RECODE` field is a state-county combination where the first two characters represent the state FIPS code and the last three digits represent the FIPS county code. This particular field illustrates an important characteristic of machine learning, that between *categorical features* and *numeric features*. All input into a machine learning algorithm must be numeric, but real numbers carry with them the usually extremely useful property known as the well-ordering property. But if one is tasked with encoding a categorical feature into suitable numeric format for machine learning, it is necessary to do so in a way that removes the well-ordering property [11].

As a simple example of how to correctly treat categorical variables in a machine learning context, consider the SEER variable `SEX`. This variable is encoded with a numeric 1 for males and a numeric 2 for females as shown in Table (1). Values such as "Male" and "Female" encoded as numbers are dangerous because if not handled properly, they can generate bogus results [12]. The proper way to transform the SEER `SEX` variable is to create two additional variables: `sex_Male` and `sex_Female`, and then to eliminate the variables `SEX` and `sex_Male` (keeping both of the variables `sex_Male` and `sex_Female` is a redundant represetation). For example,

Code	Description
1	Male
2	Female

Table 1. Encoding of gender in the SEER incidence files. These types of categorical variables need to be transformed via one-hot-encoding.

Sex		sex_Male	sex_Female		sex_Female
1	$\longrightarrow$	1	0	$\longrightarrow$	0

(2.1)

and

Sex		sex_Male	sex_Female		sex_Female
2	$\longrightarrow$	0	1	$\longrightarrow$	1

(2.2)

The procedure outlined in Equations (2.1, 2.2) is known as one-hot encoding and needs to be applied to all of the nominal categorical variables in the SEER data that we wish to include in our predictive models. In particular, in order to include the geophgraphical information contained in the SEER categorical variable `STATE-COUNTY RECODE`, it becomes necessary to create a new feature variable for each of the distinct (state,county) pairs in the data. In the United States, there are approximately 3,000 counties. Clearly, transforming the `STATE-COUNTY RECODE` data representation into distinct (state_county) columns will explode the dataset to become wider than is optimal for machine learning. Adding extra columns to your dataset, making it wider, requires more data rows (making it taller) in order for machine learning algorithms to effectively learn [11]. Because one-hot coding `STATE-COUNTY RECODE` would cause such drastic shape changes in our data, we wish to avoid doing so. Fortunately, this variable, though given as a categorical variable, is actually a recode for three ordinal variables. There is an ordering among the (state_county) columns, namely longitude, latitude, and elevation. We can transform the data in `STATE-COUNTY RECODE` into three new numerical columns: `lat`, `lng`, and `elevation`.

For example, Table (2) shows how five entries of `STATE-COUNTY RECODE` corresponding to counties within New Mexico can be represented by the `elevation`, `lat`, and `lng` features.

It is a simple exercise to construct the full lookup table from the SEER `STATE-COUNTY RECODE` variable to the corresponding three values `elevation`, `lat`, and `lng`. We use the publically available dafafile from the United States Census Bureau [13] to map the state FIPS and county FIPS codes to query strings like those in the `address` field in Table (2). It is then possible to programmatically query the Google Maps Geocoding API for the latitude and longitude [14], and the Google Maps Elevation API for the corresponding elevation [15]. An added benefit of this shift from the single categorical variable `STATE-COUNTY RECODE` to the three continuous numerical variables `lat`, `lng`,

STATE-COUNTY RECODE	address	elevation	lat	lng
35001	Bernalillo+county+NM	5207.579772	35.017785	-106.629130
35003	Catron+county+NM	8089.242628	34.151517	-108.427605
35005	Chaves+county+NM	3559.931671	33.475739	-104.472330
35006	Cibola+county+NM	6443.415570	35.094756	-107.858387
35007	Colfax+county+NM	6147.749089	36.579976	-104.472330

Table 2. Example of the transformation of `STATE-COUNTY RECODE` to `elevation` , `lat` , and `lng` .

Column	Filter
`SEQUENCE NUMBER-CENTRAL`	$\neq$ `"Unspecified"`
`AGE AT DIAGNOSIS`	$\neq$ `"Unknown age"`
`BIRTHDATE-YEAR`	$\neq$ `"Unknown year of birth"`
`YEAR OF DIAGNOSIS`	≥ 2004
`SURVIVAL MONTHS FLAG`	= `"1"`
`CS TUMOR SIZE EXT/EVAL`	$\neq$ `""`
`CS TUMOR SIZE`	$\neq 999$
`SEER RECORD NUMBER`	$= 1$
`PRIMARY SITE`	= `"LARGE INTESTINE, (EXCL. APPENDIX)"`
`SEQUENCE NUMBER-CENTRAL`	$= 0$

Table 3. Filters applied to the Colon Cancer data.

and `elevation` is that input into the web applications described in section (7) are not restricted to the states and counties coverered in the SEER registries; in fact, the input to the models can be any address you would enter into Google Maps and calls to the Google Maps Geocoding API and the Google Maps Elevation API provide the conversion from the address string to the input variables `lat` , `lng` , and `elevation` . The full lookup table analogous to Table (2) is available from a GitHub repository containing supplemental information for this study [16].

The four COLRECT.txt files were imported into a pandas DataFrame object. This data was then filtered according to the conditions in Table (3). The RESPIR.txt and BREAST.txt files were imported into separate dataframes in similar fashion and filtered according to the conditions in Table (4) and Table (5), respectively.

The following categorical features were one-hot encoded for each of the three datasets:

- `SEX` ,
- `MARITAL STATUS AT DX` ,
- `RACE/ETHNICITY` ,

Column	Filter
SEQUENCE NUMBER-CENTRAL	$\neq$ "Unspecified"
AGE AT DIAGNOSIS	$\neq$ "Unknown age"
BIRTHDATE-YEAR	$\neq$ "Unknown year of birth"
YEAR OF DIAGNOSIS	≥ 2004
SURVIVAL MONTHS FLAG	= "1"
CS TUMOR SIZE EXT/EVAL	$\neq$ ""
CS TUMOR SIZE	$\neq 999$
SEER RECORD NUMBER	$= 1$
PRIMARY SITE	= "LUNG & BRONCHUS"
SEQUENCE NUMBER-CENTRAL	$= 0$

Table 4. Filters applied to the Lung Cancer data.

Column	Filter
SEQUENCE NUMBER-CENTRAL	$\neq$ "Unspecified"
AGE AT DIAGNOSIS	$\neq$ "Unknown age"
BIRTHDATE-YEAR	$\neq$ "Unknown year of birth"
YEAR OF DIAGNOSIS	≥ 2004
SURVIVAL MONTHS FLAG	= "1"
CS TUMOR SIZE EXT/EVAL	$\neq$ " "
CS TUMOR SIZE	$\neq 999$
SEER RECORD NUMBER	$= 1$
SEQUENCE NUMBER-CENTRAL	$= 0$

Table 5. Filters applied to the Breast Cancer data.

- SPANISH/HISPANIC ORIGIN ,
- GRADE ,
- PRIMARY SITE ,
- LATERALITY ,
- SEER HISTORIC STAGE A ,
- HISTOLOGY RECODE-BROAD GROUPINGS ,
- MONTH OF DIAGNOSIS ,
- VITAL STATUS RECODE ,

and the STATE-COUNTY RECODE variable was dropped and replaced with the elevation , lat , and lng variables for all three datasets as illustrated in Table (2).

Before applying machine learning models trained with these datasets, we review in section (2.2) the sailent features of survival analysis and censored data. We then describe

in detail a method that takes full advantage of all the data, including the right-censored data, and which involves a simple and intuitive transformation, culminating in the full set of features and target variables listed in sections (A.1, A.2, A.3).

2.2 Traditional Survival Analysis

Survival analysis pertains to data containing survival times, which are *intervals* between certain kinds of events, e.g.; cancer diagnosis date and expiry date. These intervals are often affected by a kind of "partial missingness" called *censoring*. Censored data must be analyzed in a special way to avoid biased estimates and bogus conclusions. Special methods have been developed long ago to analyze censored data properly.

With survival data, including the SEER data considered in this study, you may not know the exact time of death for some subjects. Some of the SEER subjects are still alive at the the time of the latest SEER data release. When the `VITAL STATUS RECODE` variable indicates that the subject is still alive, the `SURVIVAL MONTHS` variable is only a lower bound on the true number of survival months; this is called the *date of last contact* mode of censoring. You know that each subject either died on a certain date or was definitely alive up to some last-seen date (and you don't know how far beyond that date he or she may ultimately have lived). The latter situation is called a *censored* observation.

Statisticians have developed some traditional techniques to utilize the partial information contained in censored observations: the life-table method and the Kaplan-Meier method. Both of these methods make use of the partial information to provide unbiased estimates of the two fundamental concepts: - *hazard* and *survival*, both of which are functions of time:

- **The hazard rate** $\lambda(t)$ is the probability of dying in the next small interval of time, assuming that the subject is alive right now.
- **The survival rate** $S(t)$ is the probability of living for a certain amount of time after some starting point.

Incorrect treatment of survival data still seen in practice, and leading to biased results, includes simply excluding all subjects with a censored survival time from any survival analysis, and *imputing* (replacing) the censored (last-seen) date with some reasonable value. Both of these techniques destroy the partial information contained in the censored observations and nullify the validity of the resulting estimates for the hazard rate and survival rate [2].

In 1958, Edward L. Kaplan and Paul Meier collaborated to publish the seminal paper on how to estimate the hazard and survival rates for data containing censored observations [17]. The method is straightforward and for small datasets can be performed by hand. As an example, consider the survival data shown in Table (6). In the Kaplan-Meier calculation of the survival curve, the first step is to sort the subjects in Table (6) labeled 0 through 9 by *Survival Time* in ascending order. This process results in the first two columns (*Censored Status*, and *Survival Times*) in Table (7). The *At Risk* column decreases by one for each row; in every row a subject has either been censored out of the study or has died. The hazard rate

	Survival Time (Years)	Censored Status
0	0.75	1
1	6.10	1
2	7.00	0
3	2.40	1
4	0.50	0
5	4.50	1
6	3.50	0
7	5.80	0
8	2.30	1
9	5.20	1

Table 6. Example data to illustate traditional Survival Analsyis.

	Censored Status	Survival Time	At Risk	Hazard Function	Prob of Surv	Survival Function
4	0	0.50	10	0.000000	1.000000	1.000000
0	1	0.75	9	0.111111	0.888889	0.888889
8	1	2.30	8	0.125000	0.875000	0.777778
3	1	2.40	7	0.142857	0.857143	0.666667
6	0	3.50	6	0.000000	1.000000	0.666667
5	1	4.50	5	0.200000	0.800000	0.533333
9	1	5.20	4	0.250000	0.750000	0.400000
7	0	5.80	3	0.000000	1.000000	0.400000
1	1	6.10	2	0.500000	0.500000	0.200000
2	0	7.00	1	0.000000	1.000000	0.200000

Table 7. Kaplan-Meier table corresponding to the example data in Table (6).

is then computed for each value of *Survival Time* (necessarily a discrete function because the number of subjects is countable), by dividing the value in *Censored Status* by the value in *At Risk*. The hazard function is shown in the *Hazard Function* column in Table (7). It is then straightforward to calculate the survival function; 1 - hazard function represents the probability of not dying in the next interval of time, assuming that the subject has survived up until now and is represented by column *Prob of Surv*. The cumulative survival probability can then be obtained by sucessively multiplying all these individual time-slice probabilities together. In order to survive 2.4 years, first the subject has to survive .5 years, then survive .75 years, 2.3 years and 2.4 years. The probability of surviving 2.4 years is then the product of these 3 probabilities and is given as .666 in Table(7) in the *Survival Function* column. The Kaplan-Meier survival estimate corresponding to the data given in Table (6) is shown in Table (7).

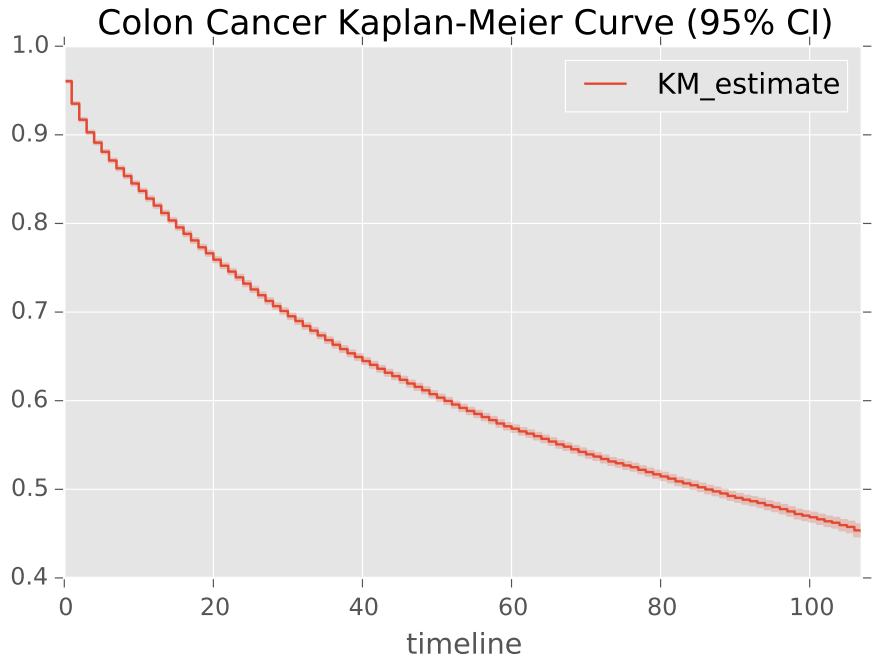

Figure 1. Traditional Kaplan-Meier estimate of the survival curve for all colon cancer patients. Fitted with 113072 observations, 71804 censored.

After the above one-hot encoding procedure, the new variable `vital_status_recode_Dead` indicates that the patient is deceased if this variable = 1, or else that the patient's record is right-censored if this variable = 0. `SURVIVAL MONTHS` and `vital_status_recode_Dead` are all that is needed to construct the Kaplan-Meier estimates for the SEER datasets. The Kaplan-Meier estimates of the survival curves for colon (Figure (1)), lung (Figure (3)), and breast cancer (Figure (2)) are constructed from the full population of cancer patients in the respective datasets. An unsatisfactory feature of these curves is that these estimates are based on populations and data with enough heterogeneity to make them not very meaningful to an indivual. Patients with very disparate characteristics are given the same prognosis by these Kaplan-Meier survival curve estimates. Therefore it is desirable to find robust predictors for survival curves of individual subjects where the input is an individual record as opposed to a population. In section (3) we present the data transformation that allows for machine learning to be applied to censored data.

3 Transformation of Censored Data for Machine Learning

In this section we describe an inuitive way to transform right-censored data appropriately so that it may be used as input to machine learning algorithms that learn the hazard fuction described in section (2.2). The full details of this transformation, and a large inspiration for this study, can be flound in this blog post [18].

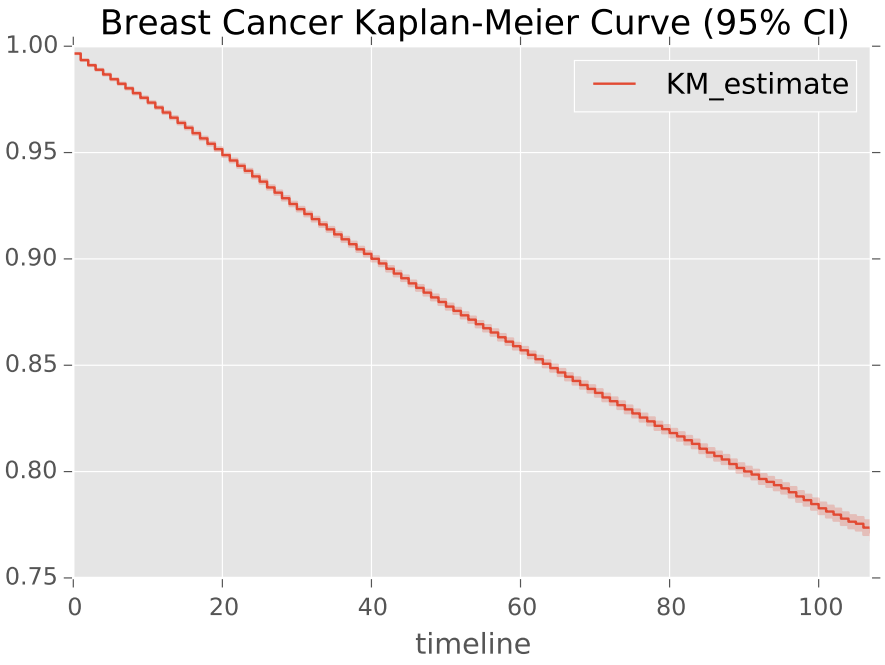

Figure 2. Traditional Kaplan-Meier estimate of the survival curve for all breast cancer patients. Fitted with 329949 observatins, 292279 censored.

The overall philosophy of the Kaplan-Meier estimate of the survival curve for a population differs fundamentally from the methods described below and used in this study. The Kaplan-Meier estimate of the survival curve is given by

$$\hat{S}(t) = \prod_{t_i<t} \frac{n_i - d_i}{n_i} \tag{3.1}$$

where d_i are the number of death events at time t and n_t is the number of subjects at risk of death just prior to time t. Equation (3.1) uses the entire data set to arrive at an estimate of the entire population survival curve. In contrast, the method described below uses the entire data set to learn a model so as to predict hazard and survival curves for all of the individual records in the data set.

The key observation is to note that the hazard function can be directly learned via standard machine learning methods. It can be rewritten as

$$\lambda(\mathbf{X}, t) = P(Y = t | Y \geq t, \mathbf{X}), \tag{3.2}$$

the probability that, if someone has survived up until month t, they will die in that month. where $\mathbf{X}$ represents all of the data for that particular record, and in our case Y represents the true, uncensored number of survival months of the patient. What is actually provided in the SEER data is the related variable `SURVIVAL MONTHS` T (how long each subject was in the study), and whether they exited by dying or being censored (D), `VITAL STATUS RECODE`. D is a Boolean variable, so $D = 1$ if $T = Y$, and $D = 0$ if $T < Y$.

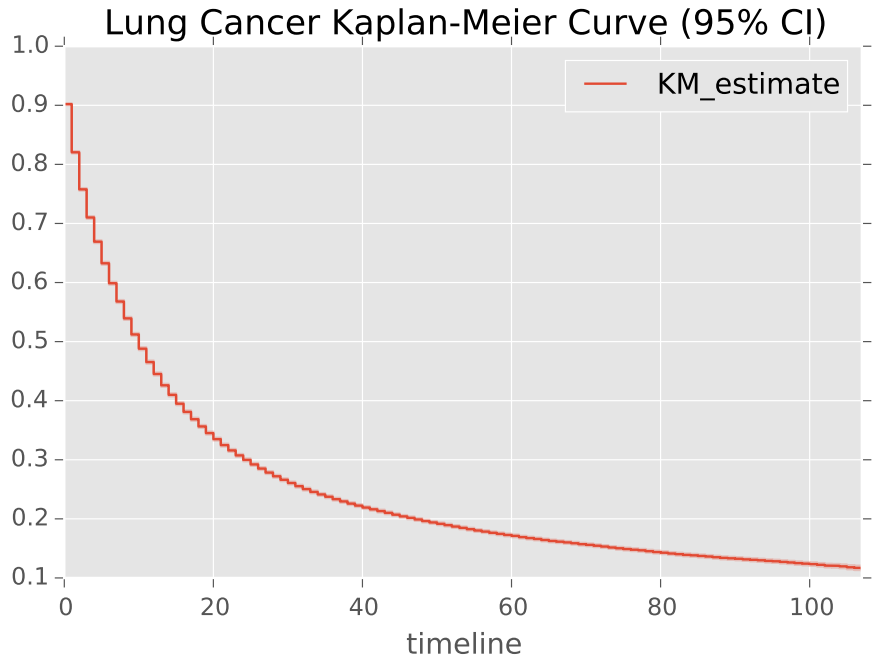

Figure 3. Traditional Kaplan-Meier estimate of the survival curve for all lung cancer patients. Fitted with 177089 observatins, 47409 censored.

In the discrete time variable case which holds for the SEER data where `SURVIVAL MONTHS` takes on integer values, the relationship between the hazard function and the survival function is given as follows [19]. Supppose that $a_j < t \leq a_{j+1}$ where a_j represents j months. Then

$$\begin{aligned} S(t) &= P(T \geq a_1, T \geq a_2, \cdots, T \geq a_{j+1}) && (3.3)\\ &= P(T \geq a_1)P(T \geq a_2 | T \geq a_1) \cdots P(T \geq a_{j+1} | T \geq a_j) && (3.4)\\ &= (1-\lambda_1) \times \cdots \times (1-\lambda_j) && (3.5)\\ &= \prod_{k:a_k<t} (1-\lambda_k) && (3.6) \end{aligned}$$

Treating T as just another covariate is the key to the transformation. Each datapoint in the hidden classification problem is the combination of an $\mathbf{X}_i$ in the orginal dataset plus some month t, and the classification problem is "did point $\mathbf{X}_i$ die in month t." We will call this new variable D_{it} (`newtarget`). We can transform our original data set into a new one, with one row for each month that each $\mathbf{X}_i$ is in the sample; train a standard classifier on this new dataset with D_{it} as the target, and derive a survival model from the orginal dataset. Psuedocode for this transformation is found in section (B).

Explicit examples will help make this transformation clear. The untransformed datapoint represented Table (8) is transformed to the multiple records shown in Table (10).

	cs_tumor_size	year_of_birth	survival_months	vital_status_recode_Dead
newindex				
205	60	1951	3	1

Table 8. Example of four columns in an uncensored record in the untransformed dataset.

	cs_tumor_size	year_of_birth	survival_months	vital_status_recode_Dead
newindex				
205	40	1950	3	0

Table 9. Example of four columns in a censored record in the untransformed dataset.

	cs_tumor_size	year_of_birth	month	newtarget
newindex				
205	60	1951	0	0
205	60	1951	1	0
205	60	1951	2	0
205	60	1951	3	1

Table 10. Example of four columns in an uncensored record in the transformed dataset.

	cs_tumor_size	year_of_birth	month	newtarget
newindex				
205	40	1950	0	0
205	40	1950	1	0
205	40	1950	2	0
205	40	1950	3	0

Table 11. Example of four columns in a censored record in the transformed dataset.

All uncensored data is transformed in this way. All censored data is similarly transformed. The untransformed datapoint represented Table (9) is transformed to the multiple records shown in Table (11).

One obvious side effect of this transformation is that it explodes the length of the dataset. For this study, the original, untransformed colon cancer DataFrame has shape $(113072, 103)$, and the total transformed colon cancer DataFrame has shape $(4165251, 103)$. Similary, the original, untransformed lung cancer DataFrame has shape $(177089, 115)$, and the total transformed lung cancer DataFrame has shape $(3079931, 115)$. The biggest ex-

plosion in dataset size occured with the breast cancer data, which is a consequence of the relatively high survival rates in breast cancer. A subject who is censored with a recorded survival months of 48 will contribute an extra 48 rows to the transformed dataset. The original, untransformed breast cancer DataFrame has shape $(329949, 67)$, and the total transformed breast cancer DataFrame has shape $(15085711, 67)$. Traning machine learning algorithms on such large datasets, even after splitting into training and testing sets described below, require large RAM. All computations for this study were performed on a Dell XPS 8700 Desktop with 32GB of RAM.

4 Training and Test Partitions

After performing the data transformation adumbrated in section (3), it is necessary to be mindful of how we partition the data into training and testing data. Each subject that was represented by a single row in the original untransformed dataset now potentially is represented by multiple rows in the transformed dataset, and care must be taken to ensure that all of the rows corresponding to a particular subject are either assigned exclusively to the training set or exclusive to the testing set. An additional characteristic of this transformed data that requires careful treatment involves balancing. The transformation results in many new records with the target variable `newtarget` $== 0$. The training and test sets must be chosen such that the ratio of the number of records with `newtarget` $== 0$ to that of the number of records with `newtarget` $== 1$ is the same in the training and test datasets. This ratio turns out to be ≈ 396 for the breast cancer data, ≈ 99 for the colon cancer data, and ≈ 22.75 for the lung cancer data. The shapes of the training and testing datasets for breast cancer used in this study are $(14936862, 67)$ and $(148849, 67)$, respectively. For lung cancer, the corresponding datasets have shapes $(2988768, 115)$ and $(91163, 115)$. Finallly, for colon cancer the partition into training and test datasets of the transformed data have the shapes $(3958008, 103)$ and $(207243, 103)$. Multiple rows correspond to the same test patient in these datasets. The colon cancer test dataset represents 5654 distinct subjects; the breast cancer test dataset represents 3300 distinct subjects; and the lung test dataset contains data for 5313 distinct subjects.

The models described below are trained to learn the values of `newtarget` , which is a binary variable: a value of '0' indicating that the subject is still alive at the given month, while a value of '1' indicates that the patient died at that particular value of `months` . The random forests and neural networks described below are binary classifiers with the target `newtarget` . Fortunately, both the random forests and neural networks are capable of not only performing strict class prediction, i.e. predicting whether `newtarget` is '0' or '1', but are also able to predict the *probablity* of `newtarget` being '0' or '1'., and thus learning the hazard function.

Finally, we emphasize the crucial point that the features `survival_months` and `vital_status_recode_Dead` are dropped from both the training and and testing data, and are replaced with the features `months` and `newtarget` , as illustrated in Tables (8, 9, 10, 11). The information of which subjects represent censored data (`vital_status_recode_Dead` $== 0$) and which died is retained and recoverable trough the `newindex` variable and is

needed for proper evaluation of the performance metrics; when evaluating AUC curves for the 6, 12, and 60 month binary classifiers, we need to limit the test data to those subjects that we know definitively whether or not they survived 6, 12 or 60 months respectively. This requirement will necessitate the elmination of some of the censored data when computing some of the performance metrics. We introduce the two machine learning algorithms used in this study below in section (5), chosen because of their high performance in machine learning competitions and their complementary methods, so that their mutual agreement on the test datasets can be taken as indication that they are actually learning useful information, which will be shown in section (6).

Random Forests are made up of an ensemble of independet **Decision trees** that are purposefully exposed to only subsets of the data. The general philosophy is presented in the popular science book "The Wisdom of Crowds" [20]. The idea is that a large number of independent non-expert opinions converge on the correct answer when averaged. The success of this philosophy of prediction was startingly shown by the success of the political and world event predictions made by the prediction market site Intrade, before its forced closure by the Commodity Futures Trading Commission [21]. The other class of methods used by IOBS to develop predictive models are called neural networks, and are modelled on how the human brain learns high level concepts from lower level ones. As opposed to the crowd-based wisdom of a random forest, a neural network is analgous to a seasoned expert. A Neural network learns from repeated exposure to the training data and improves its predictions with each pass over the data. The general philosophy is simlar to that represented by the well-known maxim that it takes 10,000 hours to become an expert in any given field [22].

5 Prediction Models

With the datasets transformed as described in section (3), we are now able to use them to train and evaluate machine learning classifiers. The classifier models described in this section are learning the hazard function: given all of the data given in sections (A.2, A.1, A.3), which includes the field `months` (the months after diagnosis), the models predict the target variable `newtarget`, which is a binary class label equal to 1 if the subject died in that month and 0 otherwise. Fortunately, both random forests and neural networks are capable of not only performing strict class prediction, i.e. predicing whether `newtarget` is 0 or 1, but are also able to predict the *probability* of `newtarget` being 0 or 1, and thus learning the hazard function. The models learn $\lambda(\mathbf{X}, \texttt{months})$. This prediction task should not be confused with the regression problem of trying to predict precisely in what month a patient will die.

The hazard functions thus learned and predicted are intermediary products; what we are really pursuing are the survival functions for each patient that are derived from the predicted hazard functions. From the resulting hazard functions for each unique patient, we can construct the resulting survival functions as presented in section (B) and Equation (3.6) and explicitly given in python code in the notebooks at the github repository containing supplemental material for this study [16]. For each subject_i, all input data minus `months`

and `newtarget` is represented by $\mathbf{X}_i$. After the classfier models have trained with target `newtarget` on the (very large) training set, each subject's survival function is computed in the corresponding (much smaller) test set. These functions are computed by using the model to predict $\lambda(\mathbf{X}_i, t_j)$ for j running from 0 to 120 months, and $\mathbf{X}_i$ corresponds to the single row corresponding to subject_i in the original untrasnformed dataset.

5.1 Decision Trees and Random Forests

Decision tree classifiers are attractive models because they can be intrepeted easily. Like the name decision tree suggests, we can think of this model as breaking down our data by making decisions based on asking a series of questions. Based on the features in our training set, the decision tree model learns a series of questions to infer the class labels of the samples.

Random forests have gained huge popularity in applications of machine learning during the last decade due to their good classification performance, scalability, and ease of use. Intuitively, a random forest can be considered as an
emphensemble of decision trees. The idea behind ensemble learning is to combine *weak learners* to build a more robust model, a *strong learner*, that has a better generalization error and is less susceptible to overfitting.

The goal behind *ensemble methods* is to combine different classifiers into a meta-classifier that has a better generalization performance than each individual classifier alone. For example, assuming that we collected predictions from 10 experts, ensemble methods would allow us to strategically combine these predictions by the 10 experts to come up with a prediction that is more accurate and robust than the predictions by each individual expert. The individual decision trees that make an ensemble are called base learners, and as long as the error rate of each base learner is less than .50, the combined random forest will benefit from the affects of combining predictions to achieve a far greater accuracy.

Figure (4) illustrates the power of ensemble methods; the Figure illustrates how the ensemble error rate is much lower than the Base learner error rate, as long as the Base learner error rate is less than 0.5. The Figure illustrates this effect for an ensemble of 500 base learners.

A big advantage of random forests is that honing in on suitable hyperparameter values (the number of trees in the forest, the depth of each decision tree, the specific measure of information gain used to choose the node splitting, etc) is not very difficult. The ensemble method is robust to noise from the individual decision trees, which helps to precent overfitting (memorizing the training dataset targets instead of generalizing from learned rules to perform successfuly on unseen data). The only parameter that has a clearly noticeable effect on performance is the number of trees to include in the forest; in general, the more trees the better the performance, but there is a price to pay in terms of computational cost. The number of trees for the forests trained in this study was relatively small, 20 trees for breast cancer and 25 for both the lung and colon cancer models.

IOBS has chosen to use the Python scikit-learn implemenation of the Random Forest machine learning classifier [23]. Random Forests are frequent winners of the Kaggle ma-

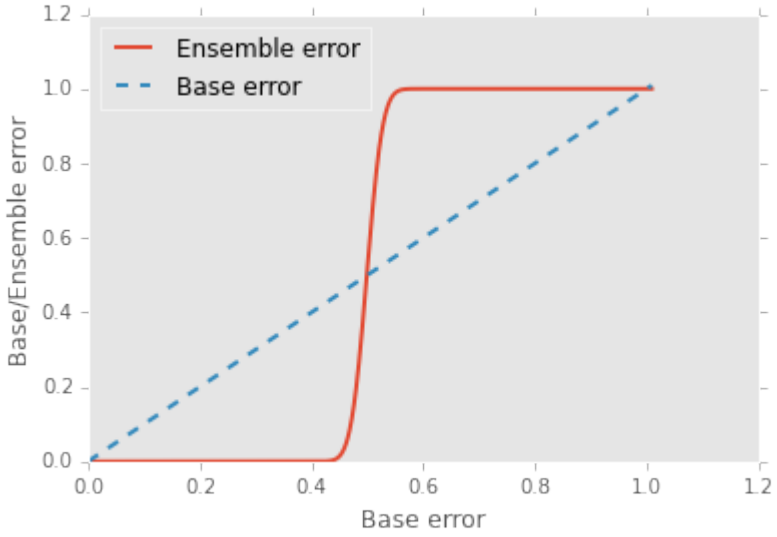

Figure 4. Illustration of ensemble methods showing how a collection of base learners with poor accuracy can combine to produce an accurate ensemble learner.

chine learning competitions [24]. The model parameters for each cancer type are given in sections (C.1, C.2, C.3).

5.2 Multi-Layer Perceptron Neural Networks

Neural networks are a biologically-inspired programming paradigm that enable computers to learn from observational data [25]. Deep learning can be understood as a set of algorithms that were developed to train artificial neural networks with many layers most efficiently. Neural networks are a hot topic not only in academic research, but also in big technology companies such as Facebook, Microsoft, and Google who invest heavily in artificial neural networks and deep learning research. As of today, complex neural networks powered by deep learning algorithms are considered as state-of-the-art when it comes to complex problem solving such as image and voice recognition. In addition, the pharmaceutical industry recently started to use deep learning techniques for drug discovery and toxicity prediction, and research has shown that these novel techniques substantially exceed the performance of traditional methods for virtual screening [26].

IOBS has chosen to use the Multi-Layer Perceptron Neural Network (MLP neural network) implementation Keras developed at MIT. Keras was initially developed as part of the research effort of project ONEIROS (Open-ended Neuro-Electronic Intelligent Robot Operating System) [27]. Keras is a minimalist, highly modular neural networks library, written in Python and capable of running on top of either TensorFlow or Theano. The model architecture for each cancer type are given in sections (C.4, C.5, C.6). Training a neural network and choosing an appropriate architecture is as much art as science [25], and the search for a good neural network architecture for the lung cancer case was more demanding than for the breast and colon.

6 Results

In order to evaluate the performance of the learned models, we first construct three binary classifiers corresponding to whether or not a subject survived 6, 12, or 60 months after diagnosis. This is done by iterating over all distinct patient indices in the test set, prediciting the full survival function, and capturing the values corresonding to 6, 12, and 60 months. If the survival function evaluted at 6 months is greater than or equal to .5 for a given subject, then the 6 months binary classifier predicts that that subject will be alive 6 months after diagnosis. Similarly, if the survival function evaluted at 60 months is less than .5, then the 12 months binary classifier predicts that that subject will be dead 12 months after diagnosis. Figure (6) illustrates the method; in this case the 6-month and 12-month classifiers predict survival, while the 60-month classifier predicts expiry.

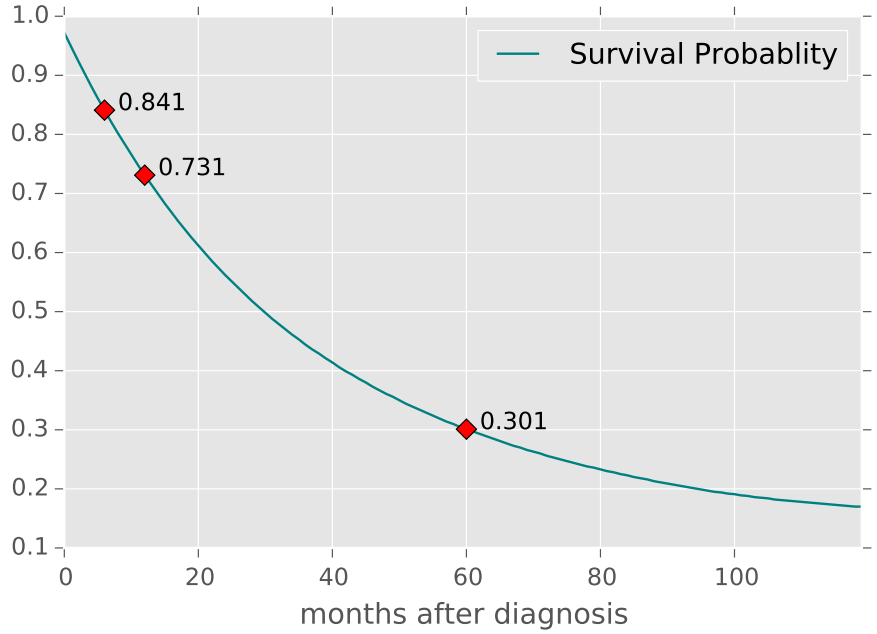

Figure 6. Example of the construction of the binary classifiers for 6, 12, and 60 months survival. A subjects hazard curve $\lambda(\mathbf{X}, t)$ is predicted by the model for times out to 120 months. The survival curve is then readily computed as in Equation (3.6). For this example, the 6-month and 12-month classifiers predict survival, while the 60-month classifier predicts expiry.

Because of censoring it is necessary to apply some Boolean filters to the data in order to correctly assess the resulting classifiers. To construct AUC curves for the 6 month classifier, we restrict ourselves to considering subjects in the test data where either of the following mutually exlusive conditions holds:

- `survival_months` $>= 6$ AND `vital_status_recode` $== 0$
- `vital_status_recode` $== 1$

Model	6 Months AUC	12 Months AUC	60 Months AUC
Breast RF	.846 (3035)	.885 (2797)	.844 (1392)
Breast NN	.855 (3035)	.867 (2797)	.836 (1392)
Colon RF	.804 (5281)	.806 (5003)	.828 (3232)
Colon NN	.797 (5281)	.804 (5003)	.841 (3232)
Lung RF	.772 (5019)	.796 (4860)	.874 (4143)
Lung NN	.765 (5019)	.796 (4860)	.875 (4143)

Table 12. AUC values for the Random Forest and Neural Networks model binary classifiers derived from the full survival curve predictions; see text for details. The number of subjects that were used in the calculation of a given AUC score are given in parenthesis after the score.

That is, we restrict ourselves to subsets of the data where we know for certain whether or not the subject survived at least 6 months. Similarly for the 12 and 60 months surivival classifiers.

6.1 Performance Metrics

The AUC scores for each of the 18 different binary classifiers are listed in Table (12). We emphasize the treatment explained in section (5) concering the correct treatment of the censored test data when evaluating performance metrics. Namely, when computing the AUC for the 12 month survival curve classifiers, we restrict the test data subjects to those that in the untransformed data set that satisfy either of the following mutually exclusive conditions:

- `survival_months` $>=$ 12 AND `vital_status_recode` $==$ 0
- `vivtal_status_recode` $==$ 1

We limit evaluation data to subsets of the data where we know for certain whether or not the subject survived at least 12 months. Similar considerations apply to the 12 and 60 months AUC calculations. The lowest AUC in Table (12) is .765, corresponding to the lung neural network model predictions for 6 months survival, while the highest AUC in Table (12) is .885, corresponding to the breast random forest model predictions for 12 months survival.

6.2 Model Agreement

An additional means of validating the predictions of these models is by comparing their predictions to each other for the same set of input data. Table (13) shows the strong agreement between the random forest and neural network classifiers for each cancer type. Python code showing how the values in Table (13) are computed is available in the files `NewPatientBreastCF.html` , `NewPatientColonCF.html` , and `NewPatientLung.html` in the GitHub repository containing supplemental matierial for this study [16]. Table (13) is computed as follows. For each cancer type (breast,colon, and lung), do the following:

Cancer Type	% agreement 6 months	% agreement 12 months	% agreement 60 months
Colon	.981	.971	.915
Breast	.994	.984	.938
Lung	.861	.883	.900

Table 13. Percentage agreement for the Random Forest and Neural Network classifiers for 6, 12, and 60 month survival predictions on the test data for each cancer type.

- use the corresponding Random Forest and Neural Network models to compute the survival curves for all of the test subjects
- extract the values of the survival curve evaluted for 6, 12, and 60 months for both models
- if both models predict less than .5 or both models predict greater than or equal to .5, that counts as agreement
- otherwise, the models disagree

The high level of agreement between two models lends confidence to the notion that they have both learned from the training data and are generalizing well. Figures (8, 7, 9) show box plots of the value of the random forest prediction subtracted from the neural network prediction. We emphasize that when evaluating the model agreement, we put no restrictions on the distinct subjects in the respective test datasets; we are confronting the models against each other, not some known ground truth as in the AUC performance metric calculations. The number of distinct subjects in all three of the colon cancer survival binary classifiers (6, 12, and 60 month survival) was 5654; for lung cancer the number of subjects entering into the calculation of Table (13) was 5313; and for breast cancer it was 3300.

7 Survival Curve Prediction Apps

The six models described in section (5), namely the random forest and MLP neural network models for each of the three cancer types considered in this study, have their full hyperparameter and architecture presented in section (C). Python code for all six model training and evaluation is available at the githib respository containing supplemental material for this study [16].

Using the popular Flask microframework for web applications [28], we have deployed these models on the Heroku Platform. Heroku is a cloud Platform-as-a-Service (PaaS) supporting several languages, including Python [29]. The list of freely accessible web applications below will hopefully allow readers not familiar with Python to experiment with the models.

1. breast cancer
   (a) random forest: http://ming-cancer.herokuapp.com/
   (b) neural network: http://breastcancer-neuralnetwork.herokuapp.com/

2. lung cancer

   (a) random forest: http://lung-cancer.herokuapp.com/
   (b) neural network: http://lungnn.herokuapp.com/

3. colon cancer

   (a) random forest: http://colon-cancer.herokuapp.com/
   (b) neural network: http://coloncancernn.herokuapp.com/

These machine learning models are used to predict survival curves for a given set of input data. The resulting surival curves predict the probablitiy that a patient with the given input data will survive at least up to month x.

For example, using the Colon Cancer neural network app, and inputing the values listed in Table (14) results in the survival curve depicted in Figure (10); the predicted probablities of living at least 6, 12, and 60 months are .89, .83, and .50, respectively.

Variable	Value
What is the tumor size (mm)	300
What is the patient's address?	boston massachusetts
Grade	moderately differentiated
Histology	adenomas and adenocarcinomas
Laterality	not a paired site
Martial Status at Dx	Single, never married
Month of Diagnosis	Jan
How many primaries	1
Race_ethnicity	White
seer_historic_stage_a	Regional
Gender	Male
spanish_hispanic_origin	Non-spanish/Non-hispanic
Year of Birth	1940
Year of Diagnosis	2010

Table 14. Example input data to the Colon Cancer neural network app http://coloncancernn.herokuapp.com/.

Changing the data in Table (14) so that the address field is changed from Boston, Massachusetts to Denver, Colorado but keeping all other variables are unchanged results in the predicted probabilities of living at least 6, 12, and 60 months: .945, .902, .665. Behind the scenes, the apps use the input to the address field to make a call to the Google Maps API to convert the address into a latitude, longitude and elevation. These probablities are noticeably higher and reflect the documented effects of both longitude and elevation on cancer treatment and prognosis in the United States [30].

Variable	Value
What is the tumor size (mm)	500
What is the patient's address?	newark new jersey
Grade	well differentiated
Histology	acinar cell neoplasms
Laterality	bilateral involvement, lateral origin unknown; stated to be single primary
Martial Status at Dx	Married including common law
Month of Diagnosis	Jan
How many primaries	1
Race_ethnicity	White
seer_historic_stage_a	Distant
Gender	Female
spanish_hispanic_origin	Non-spanish/Non-hispanic
Year of Birth	1970
Year of Diagnosis	2011

Table 15. Example input data to the Lung Cancer random forest app http://lung-cancer.herokuapp.com/.

A similar example of how changing the inputs to the models affects the predicted survival curves in interesting ways can be seen with the random forest model for lung cancer, http://lung-cancer.herokuapp.com/. Changing the data in Table (15) by toggling between male/female, and married/single four possible permutations results in the following prediction probabilites for 6, 12, and 60 month survival:

- male/married: .53, .27, .01
- male/single: .35, .18, .009
- female/married: .55, .31, .01
- female/single: .50, .27, .01

Inputting the same combinations of data into the lung cancer neural network app http://lungnn.herokuapp.com/ yields the following probabilities:

- male/married: .42, .24, .04
- male/single: .40, .22, .03
- female/married: .44, .26, .04
- female/single: .42, .24, .04

It it interesting to note that both the random forest and neural network lung cancer models predict greater 6 month survival rates for married people, with a slightly greater benefit for males than females. The effect is greater in the random forest model, but is also visible in the neural network model.

8 Further Directions

The purpose of this study has been twofold; to develop a general methodology of data transformation to survival data with censored observations so that machine learning algorithms can be applied and to help further the cause of PPPM medicine by developing models of personalized suvival curve prognosis. To help further refine the methodology, we would like to apply it to different survival datasets [31], not necessarily within the healthcare domain. In particular, the methods presented in this paper do not take into account time varying features. For example, the `cs_tumor_ size` variable that has been a part of this study is kept fixed at the value measured at diagnosis for all records corresponding to a given subject. Clearly, the actual tumor size varies along with time and a sophisitcated model can be developed to take this into account, given available datasets. Unfortunately, the SEER datasets considered in this study do not provide this kind of granularity over time.

An additional avenue of research concerns the broad concept of causality. As demonstrated in section (7), there appears to be a correlation between marital status and survival prognosis. Does this mean that if a single person in Boston, Massachusetts is diagnosed with cancer, that they should immediately get married and move to Denver? Of course not. But personal discussions with providers has confirmed for one of the authors (D.D.) that married males tend to be much more diligent in following instructions than their single counterparts. What appears to be in effect is that some of the SEER data is providing an identifiable signature of underlying causes not directly represented by the data. Latent variables not directly seen in the data are still providing echos of patterns in the data that the sheer volume allows us to see glimpses of. Marital status is in some instances a surrogate for the presence of a strong social structure and support group surrounding a patient, which presence presumably leads to more desirable survival prognosis. The daunting and exciting task of teasing out actual causality relationships within machine learning contexts has been pioneeered by Judea Pearl of the University of California, Los Angeles [4] and seems particulary relevant and applicable to censored survival data. Combining the methodlogy presented in this study for the marriage of machine learning and censored survival data with that of the pioneering work of Judea Pearl on causality will be a fruitful avenue for future research.

A Selected Features

In this Appendix we explicitly list the features chosen for each of the Colon, Breast and Lung cancer predictive models. For each cancer type, the features chosen for the random forest and neural network models were the same, so as to be best able to compare the two models. IPython notebooks explicitly providing all code, as well as html versions of the notebooks, are available from a GitHub repository providing supplemental material for thus study [16].

[4] Judea Pearl homepage at the University of California, Los Angeles, http://bayes.cs.ucla.edu/jp_home.html, accessed 11 Jan 2016.

A.1 Colon Cancer Feature Selection

The feature set used as input into both the Random Forest and Neural Network models, after the transformation described in section (3) is given below and also available in full detail in the file `NewPatientColonML.html` .

- cs_tumor_size
- elevation
- grade_cell type not determined
- grade_moderately differentiated
- grade_poorly differentiated
- grade_undifferentiated; anaplastic
- grade_well differentiated
- histology_recode_broad_groupings_acinar cell neoplasms
- histology_recode_broad_groupings_adenomas and adenocarcinomas
- histology_recode_broad_groupings_blood vessel tumors
- histology_recode_broad_groupings_complex epithelial neoplasms
- histology_recode_broad_groupings_complex mixed and stromal neoplasms
- histology_recode_broad_groupings_cystic, mucinous and serous neoplasms
- histology_recode_broad_groupings_ductal and lobular neoplasms
- histology_recode_broad_groupings_epithelial neoplasms, NOS
- histology_recode_broad_groupings_fibromatuos neoplasms
- histology_recode_broad_groupings_germ cell neoplasms
- histology_recode_broad_groupings_lipomatous neplasms
- histology_recode_broad_groupings_miscellaneous bone tumors
- histology_recode_broad_groupings_myomatous neoplasms
- histology_recode_broad_groupings_neuroepitheliomatous neoplasms
- histology_recode_broad_groupings_nevi and melanomas
- histology_recode_broad_groupings_paragangliomas and glumus tumors
- histology_recode_broad_groupings_soft tissue tumors and sarcomas, NOS
- histology_recode_broad_groupings_squamous cell neoplasms
- histology_recode_broad_groupings_synovial-like neoplasms
- histology_recode_broad_groupings_transistional cell papillomas and carcinomas
- histology_recode_broad_groupings_unspecified neoplasms
- lat
- laterality_Left: origin of primary
- laterality_Not a paired site
- laterality_Only one side involved, right or left origin unspecified
- laterality_Paired site, but no information concerning laterality; midline tumor
- laterality_Right: origin of primary
- lng
- marital_status_at_dx_Divorced
- marital_status_at_dx_Married (including common law)
- marital_status_at_dx_Separated

- marital_status_at_dx_Single (never married)
- marital_status_at_dx_Unknown
- marital_status_at_dx_Unmarried or domestic partner
- marital_status_at_dx_Widowed
- month_of_diagnosis_Apr
- month_of_diagnosis_Aug
- month_of_diagnosis_Dec
- month_of_diagnosis_Feb
- month_of_diagnosis_Jan
- month_of_diagnosis_Jul
- month_of_diagnosis_Jun
- month_of_diagnosis_Mar
- month_of_diagnosis_May
- month_of_diagnosis_Nov
- month_of_diagnosis_Oct
- month_of_diagnosis_Sep
- number_of_primaries
- race_ethnicity_Amerian Indian, Aleutian, Alaskan Native or Eskimo
- race_ethnicity_Asian Indian
- race_ethnicity_Asian Indian or Pakistani
- race_ethnicity_Black
- race_ethnicity_Chinese
- race_ethnicity_Fiji Islander
- race_ethnicity_Filipino
- race_ethnicity_Guamanian
- race_ethnicity_Hawaiian
- race_ethnicity_Hmong
- race_ethnicity_Japanese
- race_ethnicity_Kampuchean
- race_ethnicity_Korean
- race_ethnicity_Laotian
- race_ethnicity_Melanesian
- race_ethnicity_Micronesian
- race_ethnicity_New Guinean
- race_ethnicity_Other
- race_ethnicity_Other Asian
- race_ethnicity_Pacific Islander
- race_ethnicity_Pakistani
- race_ethnicity_Polynesian
- race_ethnicity_Samoan
- race_ethnicity_Thai
- race_ethnicity_Tongan
- race_ethnicity_Unknown

- race_ethnicity_Vietnamese
- race_ethnicity_White
- seer_historic_stage_a_Distant
- seer_historic_stage_a_In situ
- seer_historic_stage_a_Localized
- seer_historic_stage_a_Regional
- seer_historic_stage_a_Unstaged
- sex_Female
- spanish_hispanic_origin_Cuban
- spanish_hispanic_origin_Dominican Republic
- spanish_hispanic_origin_Mexican
- spanish_hispanic_origin_Non-Spanish/Non-hispanic
- spanish_hispanic_origin_Other specified Spanish/Hispanic origin (excludes Dominican Repuclic)
- spanish_hispanic_origin_Puerto Rican
- spanish_hispanic_origin_South or Central American (except Brazil)
- spanish_hispanic_origin_Spanish surname only
- spanish_hispanic_origin_Spanish, NOS; Hispanic, NOS; Latino, NOS
- spanish_hispanic_origin_Uknown whether Spanish/Hispanic or not
- year_of_birth
- year_of_diagnosis
- month

and `newtarget` is the target variable, indicating whether or not the subject died in month given by the value of the `month` variable.

A.2 Lung Cancer Feature Selection

The feature set used as input into both the Random Forest and Neural Network models, after the transformation described in section (3) is given below and also available in full detail in the file `NewPatientLungML.html` .

- cs_tumor_size
- elevation
- grade_cell type not determined
- grade_moderately differentiated
- grade_poorly differentiated
- grade_undifferentiated; anaplastic
- grade_well differentiated
- histology_recode_broad_groupings_acinar cell neoplasms
- histology_recode_broad_groupings_adenomas and adenocarcinomas
- histology_recode_broad_groupings_blood vessel tumors
- histology_recode_broad_groupings_complex epithelial neoplasms
- histology_recode_broad_groupings_complex mixed and stromal neoplasms

- histology_recode_broad_groupings_cystic, mucinous and serous neoplasms
- histology_recode_broad_groupings_ductal and lobular neoplasms
- histology_recode_broad_groupings_epithelial neoplasms, NOS
- histology_recode_broad_groupings_fibroepithelial neoplasms
- histology_recode_broad_groupings_fibromatuos neoplasms
- histology_recode_broad_groupings_germ cell neoplasms
- histology_recode_broad_groupings_gliomas
- histology_recode_broad_groupings_granular cell tumors & alveolar soft part sarcomas
- histology_recode_broad_groupings_lipomatous neplasms
- histology_recode_broad_groupings_miscellaneous bone tumors
- histology_recode_broad_groupings_miscellaneous tumors
- histology_recode_broad_groupings_mucoepidermoid neoplasms
- histology_recode_broad_groupings_myomatous neoplasms
- histology_recode_broad_groupings_myxomatous neoplasms
- histology_recode_broad_groupings_nerve sheath tumors
- histology_recode_broad_groupings_neuroepitheliomatous neoplasms
- histology_recode_broad_groupings_nevi and melanomas
- histology_recode_broad_groupings_osseous and chondromatous neoplasms
- histology_recode_broad_groupings_paragangliomas and glumus tumors
- histology_recode_broad_groupings_soft tissue tumors and sarcomas, NOS
- histology_recode_broad_groupings_squamous cell neoplasms
- histology_recode_broad_groupings_synovial-like neoplasms
- histology_recode_broad_groupings_thymic epithelial neoplasms
- histology_recode_broad_groupings_transistional cell papillomas and carcinomas
- histology_recode_broad_groupings_trophoblastic neoplasms
- histology_recode_broad_groupings_unspecified neoplasms
- lat
- laterality_Bilateral involvement, lateral origin unknown; stated to be single primary
- laterality_Left: origin of primary
- laterality_Not a paired site
- laterality_Only one side involved, right or left origin unspecified
- laterality_Paired site, but no information concerning laterality; midline tumor
- laterality_Right: origin of primary
- lng
- marital_status_at_dx_Divorced
- marital_status_at_dx_Married (including common law)
- marital_status_at_dx_Separated
- marital_status_at_dx_Single (never married)
- marital_status_at_dx_Unknown
- marital_status_at_dx_Unmarried or domestic partner
- marital_status_at_dx_Widowed
- month_of_diagnosis_Apr

- month_of_diagnosis_Aug
- month_of_diagnosis_Dec
- month_of_diagnosis_Feb
- month_of_diagnosis_Jan
- month_of_diagnosis_Jul
- month_of_diagnosis_Jun
- month_of_diagnosis_Mar
- month_of_diagnosis_May
- month_of_diagnosis_Nov
- month_of_diagnosis_Oct
- month_of_diagnosis_Sep
- number_of_primaries
- race_ethnicity_Amerian Indian, Aleutian, Alaskan Native or Eskimo
- race_ethnicity_Asian Indian
- race_ethnicity_Asian Indian or Pakistani
- race_ethnicity_Black
- race_ethnicity_Chamorran
- race_ethnicity_Chinese
- race_ethnicity_Fiji Islander
- race_ethnicity_Filipino
- race_ethnicity_Guamanian
- race_ethnicity_Hawaiian
- race_ethnicity_Hmong
- race_ethnicity_Japanese
- race_ethnicity_Kampuchean
- race_ethnicity_Korean
- race_ethnicity_Laotian
- race_ethnicity_Melanesian
- race_ethnicity_Micronesian
- race_ethnicity_New Guinean
- race_ethnicity_Other
- race_ethnicity_Other Asian
- race_ethnicity_Pacific Islander
- race_ethnicity_Pakistani
- race_ethnicity_Polynesian
- race_ethnicity_Samoan
- race_ethnicity_Thai
- race_ethnicity_Tongan
- race_ethnicity_Unknown
- race_ethnicity_Vietnamese
- race_ethnicity_White
- seer_historic_stage_a_Distant
- seer_historic_stage_a_In situ

- seer_historic_stage_a_Localized
- seer_historic_stage_a_Regional
- seer_historic_stage_a_Unstaged
- sex_Female
- spanish_hispanic_origin_Cuban
- spanish_hispanic_origin_Dominican Republic
- spanish_hispanic_origin_Mexican
- spanish_hispanic_origin_Non-Spanish/Non-hispanic
- spanish_hispanic_origin_Other specified Spanish/Hispanic origin (excludes Dominican Repuclic)
- spanish_hispanic_origin_Puerto Rican
- spanish_hispanic_origin_South or Central American (except Brazil)
- spanish_hispanic_origin_Spanish surname only
- spanish_hispanic_origin_Spanish, NOS; Hispanic, NOS; Latino, NOS
- spanish_hispanic_origin_Uknown whether Spanish/Hispanic or not
- year_of_birth
- year_of_diagnosis
- month

and `newtarget` is the target variable, indicating whether or not the subject died in month given by the value of the `month` variable.

A.3 Breast Cancer Feature Selection

The feature set used as input into both the Random Forest and Neural Network models, after the transformation described in section (3) is given below and also available in full detail in the file `NewPatientBreastML.html` .

- cs_tumor_size
- elevation
- grade_moderately differentiated
- grade_poorly differentiated
- grade_ndifferentiated; anaplastic
- grade_well differentiated
- histology_recode_broad_groupings_adenomas and adenocarcinomas
- histology_recode_broad_groupings_adnexal and skin appendage neoplasms
- histology_recode_broad_groupings_basal cell neoplasms
- histology_recode_broad_groupings_complex epithelial neoplasms
- histology_recode_broad_groupings_cystic, mucinous and serous neoplasms
- histology_recode_broad_groupings_ductal and lobular neoplasms
- histology_recode_broad_groupings_epithelial neoplasms, NOS
- histology_recode_broad_groupings_nerve sheath tumors
- histology_recode_broad_groupings_unspecified neoplasms
- lat

- laterality_Bilateral involvement, lateral origin unknown; stated to be single primary
- laterality_Paired site, but no information concerning laterality; midline tumor
- laterality_Right: origin of primary
- lng
- marital_stats_at_dx_Divorced
- marital_stats_at_dx_Married (inclding common law)
- marital_stats_at_dx_Separated
- marital_stats_at_dx_Single (never married)
- marital_stats_at_dx_Unknown
- marital_stats_at_dx_Unmarried or domestic partner
- marital_stats_at_dx_Widowed
- month_of_diagnosis_Apr
- month_of_diagnosis_Aug
- month_of_diagnosis_Dec
- month_of_diagnosis_Feb
- month_of_diagnosis_Jan
- month_of_diagnosis_Jul
- month_of_diagnosis_Jun
- month_of_diagnosis_Mar
- month_of_diagnosis_May
- month_of_diagnosis_Nov
- month_of_diagnosis_Oct
- month_of_diagnosis_Sep
- race_ethnicity_Amerian Indian, Aletian, Alaskan Native or Eskimo
- race_ethnicity_Asian Indian
- race_ethnicity_Black
- race_ethnicity_Chinese
- race_ethnicity_Japanese
- race_ethnicity_Melanesian
- race_ethnicity_Other
- race_ethnicity_Other Asian
- race_ethnicity_Pacific Islander
- race_ethnicity_Thai
- race_ethnicity_Unknown
- race_ethnicity_Vietnamese
- race_ethnicity_White
- seer_historic_stage_a_Distant
- seer_historic_stage_a_In sit
- seer_historic_stage_a_Localized
- seer_historic_stage_a_Unstaged
- sex_Female
- spanish_hispanic_origin_Cuban
- spanish_hispanic_origin_Mexican

- spanish_hispanic_origin_Non-Spanish/Non-hispanic
- spanish_hispanic_origin_Other specified Spanish/Hispanic origin (excldes Dominican Republic)
- spanish_hispanic_origin_Spanish surname only
- spanish_hispanic_origin_Spanish, NOS; Hispanic, NOS; Latino, NOS
- year_of_birth
- year_of_diagnosis
- month

and `newtarget` is the target variable, indicating whether or not the subject died in month given by the value of the `month` variable.

B Pseudocode for the Data Transformation

```
def train(X, T, D)
    // X, T, D are the original dataset
    X' = []
    D' = []

    // the transformation
    for each index i in X:
        for t=1 to T[i]:
            new_D = (0 if t < T[i], else D[i])
            append new_D to D'
            new_X = (X[i], t)
            append new_X to X'

    return a decision tree trained on (X', D')

def pmf(h, X)
    // X is a single datapoint
    // returns an array A where A[i] = P(Y = i | X)
    A = []
    p_so_far = 1 // this is p(T >= t | X)
    for t = 1 to (the last month where h has any data):
        // h knows p(T = t | T >= t, X), we call this p_cur
        p_cur = h's prediction for (X, t)
        append (p_so_far * p_cur) to A
        p_so_far *= (1 - p_cur)
```

C Model Architecture and Python Code

C.1 Breast Random Forest Model

```
f = RandomForestClassifier(n_estimators=20,min_samples_split=3,
                            max_depth = 15,
                           max_features = .8,
                            n_jobs=5,verbose=2,random_state=33)
```

C.2 Colon Random Forest Model

```
rf = RandomForestClassifier(n_estimators=25,min_samples_split=3,
                            max_depth = 10,
                           max_features = .5,
                            n_jobs=5,verbose=2,random_state=3)
```

C.3 Lung Random Forest Model

```
rf = RandomForestClassifier(n_estimators=25,min_samples_split=3,
                            max_depth = 11,
                           max_features = .8,
                            n_jobs=5,verbose=2,random_state=3)
```

C.4 Breast Neural Network Model

The archictecture of the Keras multilayer perceptron neural network model trained on the breast cancer data is given explicitly below:

```
modelbreast = Sequential()
modelbreast.add(Dense(114, input_shape=(66,) ,init='normal'))
modelbreast.add(Activation('relu'))
modelbreast.add(Dropout(0.05))
modelbreast.add(Dense(50, init='normal'))
modelbreast.add(Activation('relu'))
modelbreast.add(Dropout(0.05))

modelbreast.add(Dense(36, init='normal'))
modelbreast.add(Activation('relu'))
modelbreast.add(Dropout(0.05))

modelbreast.add(Dense(2, init='normal'))
modelbreast.add(Activation('softmax'))

rms = RMSprop(lr=0.001)

modelbreast.compile(loss='binary_crossentropy', optimizer=rms, class_mode="binary")
```

and trained with a batch size of 1500 for 200 epochs.

C.5 Colon Cancer Neural Network Model

The archictecture of the Keras multilayer perceptron neural network model trained on the colon cancer data is given explicitly below:

```
modelcolon = Sequential()
modelcolon.add(Dense(114, input_shape=(102,) ,init='normal'))
modelcolon.add(Activation('relu'))
modelcolon.add(Dropout(0.05))
modelcolon.add(Dense(50, init='normal'))
modelcolon.add(Activation('relu'))
modelcolon.add(Dropout(0.05))


modelcolon.add(Dense(35, init='normal'))
modelcolon.add(Activation('relu'))
modelcolon.add(Dropout(0.05))

modelcolon.add(Dense(2, init='normal'))
modelcolon.add(Activation('softmax'))

rms = RMSprop(lr=0.001)

modelcolon.compile(loss='binary_crossentropy', optimizer=rms, class_mode="binary")
```

and trained with a batch size of 1500 for 200 epochs.

C.6 Lung Cancer Neural Network Model

The archictecture of the Keras multilayer perceptron neural network model trained on the lung cancer data is given explicitly below:

```
modellung = Sequential()
modellung.add(Dense(114, input_shape=(114,) ,init='normal'))
modellung.add(Activation('relu'))
modellung.add(Dropout(0.1))
modellung.add(Dense(80, init='normal'))
modellung.add(Activation('relu'))
modellung.add(Dropout(0.1))
modellung.add(Dense(40, init='normal'))
modellung.add(Activation('relu'))
```

```
modellung.add(Dropout(0.1))


modellung.add(Dense(2, init='normal'))
modellung.add(Activation('softmax'))


rms = RMSprop(lr=0.001)

modellung.compile(loss='binary_crossentropy', optimizer=rms, class_mode="binary")
```

and trained with a batch size of 2000 for 50 epochs.

Acknowledgments

This is the most common positions for acknowledgments. A macro is available to maintain the same layout and spelling of the heading.

Note added. This is also a good position for notes added after the paper has been written.

References

[1] Sebastian Raschka, *Python Machine Learning Essentials*. Packt Publishing, 2015.

[2] Cam Davidson-Pilon, "Quickstart – lifelines 0.8.0.1 documentation." http://lifelines.readthedocs.org/en/latest/Quickstart.html, 2016 (accessed 14 Jan 2016).

[3] S. Van Poucke, Z. Zhang, M. Schmitz, M. Vukicevic, M. Laenen, L. Celi, and C. De Deyne, "Scalable predictive analysis in critically ill patients using a visual open data analysis platform," *PLoS ONE*, vol. 11, no. 1, 2016. cited By 0.

[4] National Cancer Institute, the Surveillance, Epidemiology, and End Results Program, "About the SEER Program - SEER." http://seer.cancer.gov/about, 2016 (accessed 14 Jan 2016).

[5] Shin, Hyunjung and Nam, Yonghyun, "A coupling approach of a predictor and a descriptor for breast cancer prognosis," *BMC MEDICAL GENOMICS*, vol. 7, MAY 8 2014. 3rd Annual Translational Bioinformatics Conference (TBC) / ISCB-Asia, Seoul, SOUTH KOREA, OCT 02-04, 2013.

[6] Zolbanin, Hamed Majidi and Delen, Dursun and Zadeh, Amir Hassan, "Predicting overall survivability in comorbidity of cancers: A data mining approach," *DECISION SUPPORT SYSTEMS*, vol. 74, pp. 150–161, JUN 2015.

[7] L. Gordon and R. Olshen, "Tree-structured survival analysis," *Cancer Treatment Reports*, vol. 69, no. 10, pp. 1065–1068, 1985. cited By 97.

[8] I. Bou-Hamad, D. Larocque, and H. Ben-Ameur, "A review of survival trees," *Statistics Surveys*, vol. 5, pp. 44–71, 2011. cited By 15.

[9] H. Ishwaran and U. Kogalur, "Consistency of random survival forests," *Statistics and Probability Letters*, vol. 80, no. 13-14, pp. 1056–1064, 2010. cited By 26.

[10] National Cancer Institute, the Surveillance, Epidemiology, and End Results Program, "Documentation for ASCII Text Data Files - SEER Datasets." http://seer.cancer.gov/data/documentation.html, 2016 (accessed 15 Jan 2016).

[11] Michael Bowles, *Machine Learning in Python: Essential Techniques for Predictive Analysis.* Wiley, 2015.

[12] Allen Downey, *Think Stats.* O'Reilly Media, 2014.

[13] United States Census Bureau, "2010 fips code files for counties - geography - u.s. census bureau." https://www.census.gov/geo/reference/codes/cou.html, 2016 (accessed 18 Jan 2016).

[14] Google Developers, "The google maps geocoding api | google maps geocoding api | google developers." https://developers.google.com/maps/documentation/geocoding/intro, 2016 (accessed 18 Jan 2016).

[15] Google Developers, "The google maps elevation api | google maps elevation api | google developers." https://developers.google.com/maps/documentation/elevation/intro?hl=en, 2016 (accessed 18 Jan 2016).

[16] IOBS, "Supplemental material | paperdata." https://github.com/doolingdavid/PAPERDATA.git, 2016 (accessed 18 Jan 2016.

[17] E. Kaplan and P. Meier, "Nonparametric estimation from incomplete observations," *Journal of the American Statistical Association*, vol. 53, no. 282, pp. 457–481, 1958. cited By 34216.

[18] Ben Kuhn, "Decision trees for survival analysis." http://www.benkuhn.net/survival-trees, 2016 (accessed 14 Jan 2016).

[19] Northeastern Illinois Chapter, American Statistical Association, "Survival analysis: Introduction." http://www.amstat.org/chapters/northeasternillinois/pastevents/presentations/summer05_Ibrahim_J.pdf, 2005 (accessed 27 Jan 2016).

[20] James Surowiecki, *The Wisdom of Crowds.* Doubleday, 2004.

[21] John Cassidy, "What killed Intrade?." http://www.newyorker.com/news/john-cassidy/what-killed-intrade, 13 Mar 2013 (accessed 25 Jan 2016).

[22] Malcolm Gladwell, *Outliers.* Back Bay Books, 2011.

[23] scikit-learn developers, "3.2.4.3.1. sklearn.ensemble.randomforestclassifier." http://scikit-learn.org/stable/modules/generated/sklearn.ensemble.RandomForestClassifier.html, 2014 (accessed 25 Jan 2016).

[24] Kaggle Inc., "Random forests | kaggle." https://www.kaggle.com/wiki/RandomForests, 2015 (accessed 25 Jan 2016.

[25] Michael Nielsen, "Neural networks and deep learning." http://neuralnetworksanddeeplearning.com/, Jan 2016 (accessed 25 Jan 2016).

[26] T. Unterthiner, A. Mayr, G. Klambauer, and S. Hochreiter, "Toxicity prediction using deep learning." http://arxiv.org/abs/1503.01445, 4 Mar 2015 (accessed 25 Jan 2016).

[27] François Chollet, "Keras documentation." http://keras.io/, 2015 (accessed 25 Jan 2016).

[28] Armin Ronacher, "Welcome | Flask (A Python Microframework), howpublished=http://flask.pocoo.org/, year="2014 (accessed 29 jan 2016)"."

[29] Heroku, "Heroku | Home." https://www.heroku.com/home, 2016 (accessed 29 Jan 2016).

[30] Kai Porter, KOB Eyewitness News 4, "Study links higher elevation with lower lung cancer risk." http://www.kob.com/article/stories/s4029233.shtml#.VqlUafkrJhF, 26 Jan 2016 (accessed 27 Jan 2016).

[31] Statistical Software Information, University of Massachusetts Amherst, "Software - statistical consulting center - umass amherst." https://www.umass.edu/statdata/statdata/stat-survival.html, 2004 (accessed 29 Jan 2016).

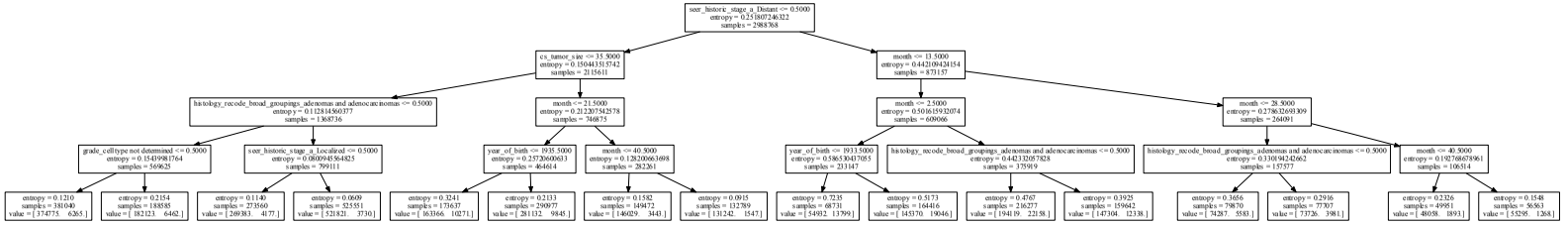

Figure 5. The top levels of a decision tree trained on the Lung Cancer training data.

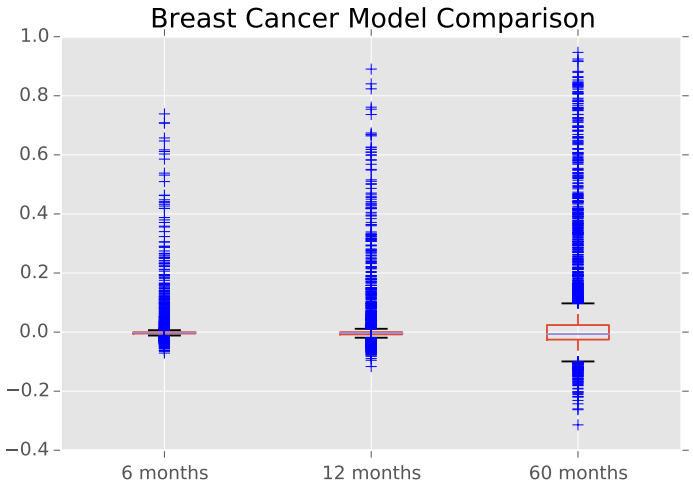

Figure 7. Box plots showing the distributions of the signed difference between the MLP model's prediction for the probability of surviving 6 months and the Random Forest model's prediction of the same quantity for breast cancer. The plot shows the same quantity for the 12 and 60 months classifiers. It is apparent from the figures that the outliers are due to the neural network models predicting higher survival probablitlies than the random forest for some few cases. These differences were evaluated for the 3300 test patients in the breast cancer data.

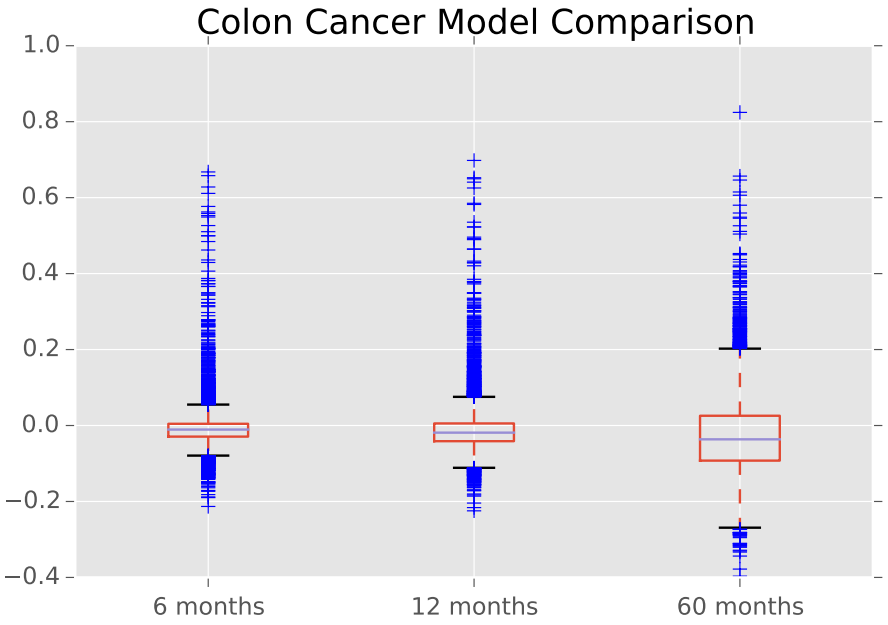

Figure 8. Box plots showing the distributions of the signed difference between the MLP model's prediction for the probability of surviving 6 months and the Random Forest model's prediction of the same quantity for colon cancer. The plot shows the same quantity for the 12 and 60 months classifiers. It is apparent from the figures that the outliers are due to the neural network models predicting higher survival probablitlies than the random forest for some few cases. These differences were evaluated for the 5654 test patients in the colon cancer data.

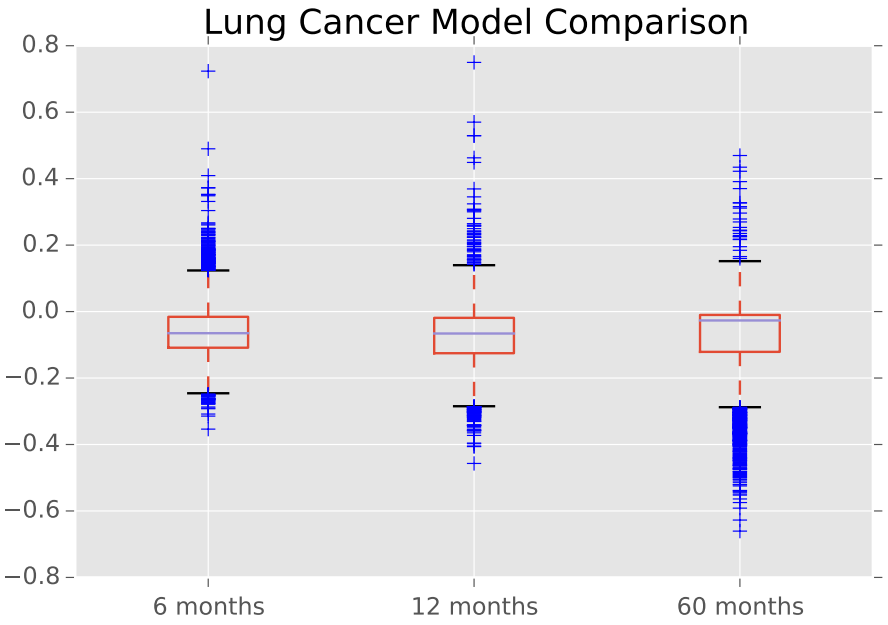

Figure 9. Box plots showing the distributions of the signed difference between the MLP model's prediction for the probability of surviving 6 months and the Random Forest model's prediction of the same quantity for lung cancer. The plot shows the same quantity for the 12 and 60 months classifiers. These differences were evaluated for the 5313 test patients in the lung cancer data. The Interquartile Ranges for lung cancer are visibly larger than those for breast cancer and colon cancer shown in fig 7 and fig 8.

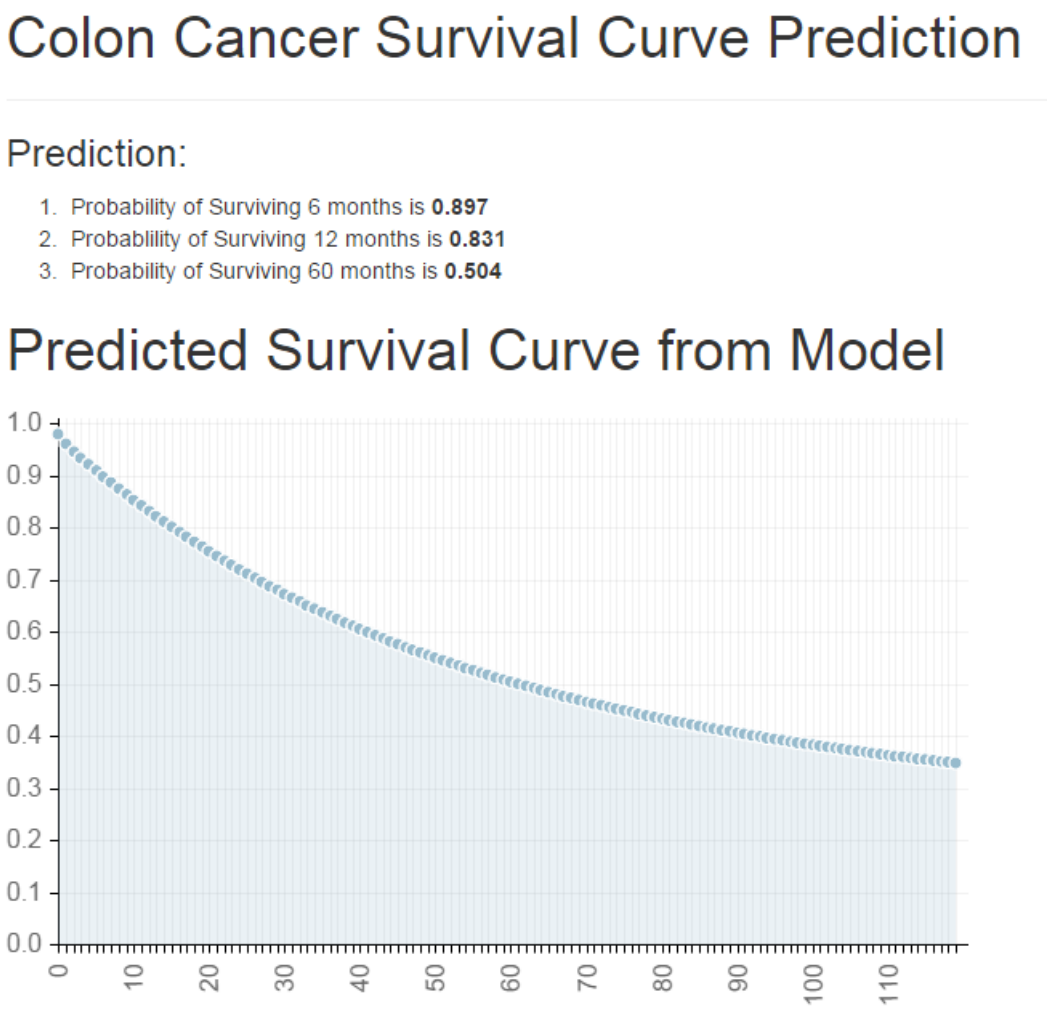

Figure 10. Colon Cancer Survival Curve predicted from the data in Table (14) using the neural network web app http://coloncancer.herokuapp.com/.